Articles

Structural Investigations on the Coordination Environment of the Active-Site Copper Centers of Recombinant Bifunctional Peptidylglycine α-Amidating Enzyme†

John S. Boswell,‡ Brian J. Reedy,‡ Raviraj Kulathila,§,|| David Merkler,§,⊥ and Ninian J. Blackburn*,‡

Department of Chemistry, Biochemistry, and Molecular Biology, Oregon Graduate Institute of Science & Technology, P.O. Box 91000, Portland, Oregon 97291-1000, and Unigene Laboratories, 110 Little Falls Road, Fairfield, New Jersey 07004

Received March 27, 1996; Revised Manuscript Received June 24, 1996⊗

ABSTRACT: The structure and coordination chemistry of the copper centers in the bifunctional peptidylglycine α-amidating enzyme (α-AE) have been investigated by EPR, EXAFS, and FTIR spectroscopy of a carbonyl derivative. The enzyme contains 2 coppers per 75 kDa protein molecule. Double integration of the EPR spectrum of the oxidized enzyme indicates that 98 ± 13% of the copper is EPR detectable, indicating that the copper centers are located in mononuclear coordination environments. The Cu(II) coordination of the oxidized enzyme is typical of type 2 copper proteins. EXAFS data are best interpreted by an average coordination of 2−3 histidines and 1−2 O/N (probably O from solvent, Asp or Glu) as equatorial ligands. Reduction causes a major structural change. The Cu(I) centers are shown to be structurally inequivalent since only one of them binds CO. EXAFS analysis of the reduced enzyme data indicates that the non-histidine O/N shell is displaced, and the Cu(I) coordination involves a maximum of 2.5 His ligands together with 0.5 S/Cl ligand per copper. The value of ν(CO) (2093 cm^{-1}) derived from FTIR spectroscopy suggests coordination of a weak donor such as methionine, which is supported by a previous observation that the ΔPro-PHM382s mutant $M^{314}I$ is totally inactive. Binding of the peptide substrate N-Ac-Tyr-Val-Gly causes minimum structural perturbation at the Cu(I) centers but appears to induce a more rigid conformation in the vicinity of the S-Met ligand. The unusually intense 8983 eV Cu K-absorption edge feature in reduced and substrate-bound-reduced enzymes is suggestive of a trigonal or digonal coordination environment for Cu(I). A structural model is proposed for the copper centers involving 3 histidines as ligands to Cu^I_A and 2 histidines and 1 methionine as ligands to Cu^I_B. However, in view of the intense 8934 eV edge feature and the lack of CO-binding ability, a 2-coordinate structure for Cu_A is also entirely consistent with the data.

C-Terminal peptide amidation is essential for the bioactivity of numerous peptide hormones involved in the regulation and control of cellular function. The amidation reaction is carried out by the bifunctional enzyme peptidylglycine α-amidating monooxygenase (PAM,[1] EC 1.14.17.3) according to the reaction chemistry below.

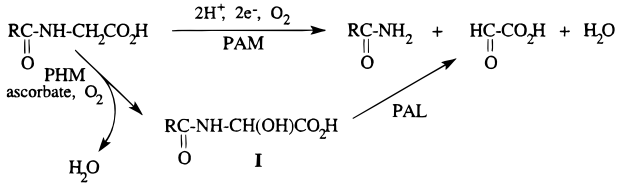

The reaction involves two separate activities involving (i) C_α hydroxylation of the terminal glycine residue to form the intermediate peptidyl α-hydroxyglycine, **I** [peptidylglycine α-hydroxylating monooxygenase (PHM) activity], and (ii) elimination of water coupled to N−C bond fission to form an amidated peptide and glyoxalate [peptidyl α-hydroxyglycine α-amidating lyase (PAL) activity]. Both activities are encoded by a single gene which can produce different (i.e., tissue-specific) forms of the enzyme via alternate splicing and endoproteolytic posttranslational processing (Stoffers et al., 1989). The full-length mRNA encodes a membrane-bound, 120 kDa bifunctional protein comprised of an NH_2-terminal PHM domain, a PAL domain, a hydrophobic transmembrane (membrane-anchoring) domain, and a cytoplasmic tail, as shown in Figure 1. However, mRNAs which lack either of the optional exons A and B encode lower-molecular mass species and undergo further

† This work was supported by a grant from the National Institutes of Health (NS27583) to N.J.B. We gratefully acknowledge the use of facilities at the Stanford Synchrotron Radiation Laboratory, which is supported by the National Institutes of Health Biomedical Research Technology Program, Division of Research Resources, and by the Department of Energy, Office of Health and Environmental Research. We are also grateful to the Collins Foundation for the purchase of the FTIR spectrometer.

‡ Oregon Graduate Institute of Science & Technology.

§ Unigene Laboratories.

|| Present address: Biophysical Chemistry Group, Pharmaceutical Division, Ciba-Geigy, 556 Morris Ave., Summit, NJ 07901.

⊥ Present address: Department of Biochemistry, Duquesne University, Pittsburgh, PA 15282.

⊗ Abstract published in *Advance ACS Abstracts,* August 15, 1996.

[1] Abbreviations: α-AE, α-amidating enzyme; Dβ*M*, dopamine β-monooxygenase; deoxyHC, deoxyhemocyanin; EXAFS, extended X-ray absorption fine structure; FI, fit index; FTIR, Fourier transform infrared; MS, multiple scattering; PAL, peptidyl α-hydroxyglycine α-amidating lyase; PAM, peptidylglycine α-amidating monooxygenase; PHM, peptidylglycine α-hydroxylating monooxygenase; XAS, X-ray absorption spectroscopy.

S0006-2960(96)00742-8 CCC: $12.00

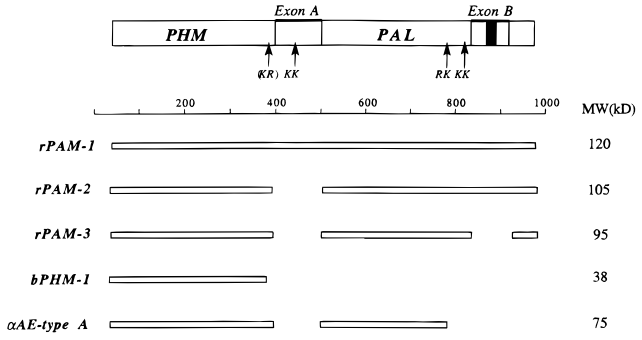

FIGURE 1: Different PAM molecules produced by alternate splicing. The coding regions of the PAM gene are represented by the rectangular box at the top of the diagram and show PHM and PAL coding domains, the regions encoding optional exons A and B, and the putative membrane-anchoring coding region (black-shaded area). The different mRNAs produced by alternate splicing are represented by the rectangular boxes in the lower portion of the figure, together with the molecular mass (kDa) of the molecule they encode. Coding regions are drawn to scale relative to amino acid residues 1−1000.

endoproteolytic processing at paired basic amino acid sites, which are contained within the exon coding sequence (Eipper et al., 1991, 1992; Husten & Eipper, 1991; Husten et al., 1993; Stoffers et al., 1991). Thus, for example, rPAM-1 and rPAM-2 (the major forms of PAM in rat atrium) are membrane-associated bifunctional proteins, since both contain the membrane-anchoring domain encoded by exon B (Husten & Eipper, 1991). On the other hand, rPAM-3, the major bifunctional form found in neurointermediate pituitary and in brain, lacks exon B and is a soluble protein (Stoffers et al., 1991). Similarly, mRNAs which contain the optional exon A encode proteins which are generally processed to monofunctional forms which exhibit separate PHL or PAL activities. Two forms of PHM, bPHM-A (38 kDa) and bPHM-B (54 kDa), have been isolated from bovine pituitary and result from proteolytic cleavage at $Lys^{383}Arg^{384}$ (absent in rat) and $Lys^{432}Lys^{433}$, while further proteolytic cleavage at $Lys^{821}Lys^{822}$ generates the 50 kDa monofunctional PAL fragment (Eipper et al., 1991; Stoffers et al., 1991). A similar distribution of bifunctional and monofunctional activities has been reported for the amidating enzymes isolated from frog skin (Iwasaki et al., 1991, 1993; Shimoi et al., 1992; Suzuki et al., 1993). Recent work from a number of laboratories has led to the overexpression of full-length and truncated bifunctional forms of the enzyme (retaining both catalytic activities) as well as monofunctional forms which exhibit separate PHM or PAL activity (Eipper et al., 1995; Husten et al., 1993; Merkler & Young, 1991; Milgram et al., 1992; Miller et al., 1992; Shimoi et al., 1992; Suzuki et al., 1993).

The PHM domain has strong similarities to the catecholamine biosynthetic enzyme dopamine β-monooxygenase (DβM) (Blackburn, 1993; Stewart & Klinman, 1988). Both enzymes are copper/ascorbate-dependent monooxygenases, with an unusual sensitivity to inactivation by H_2O_2 (Eipper et al., 1983; Merkler et al., 1992b). Approximately 30% sequence homology exists between the two enzymes, which has allowed prediction of important catalytic residues (Eipper et al., 1995; Southan & Kruse, 1989). Intrachain disulfide linkages in DβM correspond to conserved Cys residues, indicating a similar polypeptide fold in the catalytic core of the two enzymes (Robertson et al., 1994). Like DβM, PHM activity has a requirement for 2 copper atoms (Eipper et al., 1995; Kulathila et al., 1994), which undergo redox cycling during the catalytic mechanism (Freeman et al., 1993), and produces a hydroxylated product in which the oxygen atom is derived exclusively from O_2 (Merkler et al., 1992a; Noguchi et al., 1992; Zabriskie et al., 1991).

Given the strong similarities between DβM and the PHM domain, we have embarked on detailed comparative spectroscopic studies aimed at establishing the relationship between coordination chemistry and catalytic function in this class of copper monooxygenases. Extensive spectroscopic studies on DβM have led to the formulation of an active-site model in which the 2 copper centers are structurally and functionally inequivalent (Cu_A and Cu_B) (Blackburn et al., 1990, 1991; Pettingill et al., 1991; Reedy & Blackburn, 1994). In the oxidized enzyme, both Cu(II) centers appear to be tetragonal and ligated to 2−3 histidines per copper and 1−2 O donors (probably from solvent). However, reduction to the Cu(I) dioxygen-binding form of the enzyme results in a dramatic structural change, the most notable feature of which is the appearance of an S donor coordinated to one of the Cu(I) centers. CO binding experiments and X-ray absorption spectroscopy of the carbonyl derivatives of fully metallated and Cu_A-depleted forms have shown that CO (and, by inference, O_2) binds specifically at the Cu_B center, which also contains the coordinated S donor ligand.

Our initial efforts to investigate the coordination chemistry of the copper centers in the amidating enzyme focused on a recombinant (rat) monofunctional PHM construct, PHMsΔPro, modeled on the shortest catalytically active, naturally occurring PHM molecule, bPAM-A, which terminates at residue 382 (Eipper et al., 1995). Biosynthetic labeling and activity measurements on a series of truncation mutants of this construct indicated a catalytic core that did not extend past Asp^{359}. Site-directed mutagenesis further indicated that 2 histidine residues (H^{108} and H^{244}) and 1 methionine (M^{314}) were absolutely essential for catalysis and were most likely copper ligands, while a tyrosine (Y^{79}), though not a copper ligand, was predicted to be close to the active site and was probably involved in substrate binding or some other catalytic function.

In the present paper, we explore the copper coordination chemistry of the recombinant bifunctional α-amidating enzyme (α-AE) type A form of the enzyme [cloned from rat medullary thyroid carcinoma (CA-77) cells and expressed in a stable CHO cell line (Miller et al., 1992)]. The mRNA encoding this form of the enzyme in CA-77 cells contains exon B but not exon A. Although initially synthesized as a full-length, membrane-bound protein, proteolytic processing eventually generates a stable 75 kDa bifunctional form which does not undergo further cleavage to separate PHM and PAL activities (Bertelsen et al., 1990). Therefore, the recombinant bifunctional α-AE type A protein was constructed to terminate at Val^{715}, the residue immediately preceding the putative site of proteolytic cleavage ($Lys^{716}Lys^{717}$). Here we report results of EPR, EXAFS, and FTIR, which firmly establish the structural similarity of the copper centers in the PHM domain to those of DβM. In particular, the observation of a prominent feature attributable to S coordination to Cu(I) in reduced bifunctional α-AE, coupled with our earlier demonstration of the essential catalytic role of Met^{314}, establishes the novel coordination of a methionine residue at the dioxygen-binding center of this class of copper monooxygenases.

MATERIALS AND METHODS

Enzyme Isolation. Chinese hamster ovary cells which secrete recombinant type A rat medullary thyroid carcinoma α-AE into the culture medium were grown in a Wheaton stirred tank bioreactor (Matthews et al., 1994). The bifunctional 75 kDa enzyme was purified as described by Miller et al. (1992) except that the final gel filtration step (Sephacryl S-300) was carried out using 20 mM HEPES/NaOH (pH 7.8), 50 mM NaCl, and 0.001% (v/v) Triton X-100. The purified α-AE was ≥95% pure as judged by SDS−PAGE and had a specific activity of 7.8 μmol min^{-1} mg^{-1}.

Activity Determination. The conversion of dansyl-Tyr-Val-Gly to dansyl-Tyr-Val-NH_2 was monitored by isocratic elution from a C_{18} reverse-phase HPLC column (4.6 × 100 mm, Keystone Scientific Hypersil ODS) as previously described (Jones et al., 1988). Standard assays to screen column fractions and to determine specific activity were carried out at 37 °C by the addition of enzyme into 100 mM MES/KOH (pH 6.0), 30 mM KCl, 30 mM KI, 1 μM $CuSO_4$, 100 μg/mL catalase, 1% (v/v) ethanol, 0.001% (v/v) Triton X-100, 20 μM dansyl-Tyr-Val-Gly, and 10 mM ascorbate. Ethanol was added to protect the catalase against ascorbate-mediated inactivation (Davison et al., 1986), and Triton X-100 was included to prevent the nonspecific absorption of the enzyme to the sides of the tubes. At regularly timed intervals, an aliquot (50 μL) was removed, added to 10 μL of 6% (v/v) trifluoroacetic acid to quench the reaction, and then applied to the HPLC column for analysis of the percent conversion of dansyl-Tyr-Val-Gly to dansyl-Tyr-Val-NH_2. Oxygen consumption was measured using a Yellow Springs Instrument Model 53 monitor. One unit of α-AE is the amount of enzyme necessary to convert 1 μmol of dansyl-Tyr-Val-Gly to dansyl-Tyr-Val-NH_2 (or consume 1 μmol of O_2) in 1 min under the standard conditions.

Reconstitution with ^{63}Cu and Preparation of Fully Oxidized Enzyme. As isolated, the bifunctional α-AE was approximately 90% apoprotein as determined by flame atomic absorption. Consequently, the enzyme was reconstituted with Cu^{2+} prior to spectroscopic measurement. Pure isotope (^{63}Cu) was used in the reconstitution protocol in order to sharpen the EPR lines. The sample [16.7 mg/mL, 50 mM sodium HEPES, 20 mM NaCl (pH 7.8)] was first washed three times in an Amicon "centricon" ultrafiltration cell with 50 mM potassium phosphate buffer (pH 7.4) by diluting to 2 mL with the phosphate buffer and then concentrating to 500 μL. Two molar equivalents of ^{63}Cu was added to the final concentrate (1.5 mL of 294 μM ^{63}Cu added to 550 μL of the apoenzyme), and the sample was incubated on ice for 10 min. It was then concentrated to 400 μL and washed with 2 mL of 50 mM potassium phosphate (pH 7.4) containing 5 μM $^{63}Cu^{2+}$ (to remove any excess copper).

Preparation of Reduced Enzyme. A 220 μL sample of the oxidized reconstituted enzyme was made anaerobic by repeated vacuum flushing with pure argon. It was then reduced with a 5-fold excess of sodium ascorbate (10 μL of stock sodium ascorbate in 50 mM phosphate buffer at pH 7.4). Glycerol was then added to 20% (v/v). Fifty microliters of this solution was transferred anaerobically to an EXAFS cell and frozen immediately in liquid N_2.

Preparation of the CO Derivative and Measurement of the CO Binding Stoichiometry. The remainder of the reduced sample prepared above was transferred to one chamber of an airtight, double-chamber apparatus with the second chamber containing the identical buffer used in the preparation of the enzyme (50 mM potassium phosphate at pH 7.4) as a control (Reedy & Blackburn, 1994). Both chambers of the apparatus were equilibrated with the same partial pressure of CO gas (1−1.3 atm). Under these conditions, the reduced enzyme reacts completely with CO. The stoichiometry of CO binding was determined by titrating with deoxyhemoglobin in the presence of the O_2-scavenging system ascorbate/ascorbate oxidase as previously described in detail (Reedy & Blackburn, 1994).

Table 1: Experimental Parameters Used in Data Collection

	oxidized	reduced	substrate-bound
synchrotron source		SSRL	
beam energy (GeV)		3.0	
stored current range (mA)		110−40	
beam line		7.3	
harmonic rejection		mono detuned 50%	
monochromator		Si(220)	
energy range (eV)	8750−9608	8750−9608	8750−9599
energy resolution (eV)		0.5−1	
upstream slit (mm)		1.2 −1.0	
hutch aperture slit (mm)		1.2−0.8	
detector		13-element Ge	
max count rate (kHz)		35	
dead time correction		no	
number of scans	17	25	31
E_0 (start of EXAFS) (eV)		8985	

Preparation of Substrate-Bound Reduced Enzyme. Another sample of oxidized enzyme [reconstituted by the procedure described above, 20% glycerol (v/v)] was reduced with a 5-fold excess of ascorbate and then reacted with a 2-fold excess of the peptide substrate N-acetyl-Tyr-Val-Gly. Since the K_m for this substrate with the bifunctional enzyme is 6−14 μM (Husten et al., 1993; Miller et al., 1992), an excess concentration of peptide of 2 mM should ensure stoichiometric binding of substrate to the enzyme. The substrate-bound sample (50 μL) was transferred anaerobically to an EXAFS cell and frozen immediately.

EPR Measurements. EPR spectra were recorded on a Varian E109 X-band spectrometer operating at approximately 9.1 GHz. Samples were measured as frozen glasses in 20−25% glycerol (v/v) at temperatures of 120−140 K. Data were collected, averaged, and integrated using the program IGOR (Wavemetrics) running on a Macintosh Quadra 650 computer interfaced to the spectrometer. Cu^{2+} concentrations were estimated by comparison of the double integrals of the enzyme samples to Cu(II)−EDTA standard solutions (200−1000 μM) measured in the same quartz tube.

Fourier Transform Infrared (FTIR) Measurements. FTIR spectra were recorded on a Perkin-Elmer 2000 FTIR spectrophotometer. Solution IR protein spectra (200 scans) were collected at 10 °C in a 50 μm path-length calcium fluoride cell, using a liquid nitrogen-cooled MCT detector. Reported spectra are differences of CO-bound and CO-free reduced enzyme, measured under identical conditions. A nominal instrumental resolution of 2 cm^{-1} was employed.

X-ray Absorption (XAS) Data Collection and Analysis. XAS data were collected at the Stanford Synchrotron Radiation Laboratory (SSRL) on beam line 7.3. Experimental conditions are summarized in Table 1. The protein samples were measured as frozen glasses in 20% glycerol at 11−14 K in fluorescence mode using a 13-element Ge

detector. To avoid detector saturation, the count rate of each detector channel was kept below 35 kHz by adjusting the hutch entrance slits or by moving the detector in or out from the cryostat windows. Under these conditions, no dead time correction was necessary. The summed data for each detector were then inspected, and only those channels that gave high-quality backgrounds free from glitches, dropouts, or scatter peaks were included in the final average. Raw data were averaged, background subtracted, and normalized to the smoothly varying background atomic absorption using the EXAFS data reduction package EXAFSPAK (George, 1990). The experimental energy threshold ($k = 0$) was chosen as 8985 eV. Energy calibration was achieved by reference to the first inflection point of a copper foil (8980.3 eV) placed between the second and third ion chambers. In any series of scans, the measured energy of the first inflection of the copper foil spectrum varied by less than 1 eV. Averaged EXAFS data were referenced to the copper calibration of the first scan of a series, since the energy drift in any series of scans was too small to perturb the EXAFS oscillations. However, for edge studies, there was sufficient energy drift over the duration of the scans to lead to artifactual broadening of the edge features. To avoid this, edge data were generated from single scans and calibrated directly from the copper foil spectrum corresponding to that scan.

Data analysis was carried out by least-squares curve fitting utilizing full curved-wave calculations as formulated by the SRS library program EXCURV (Binsted et al., 1988; Gurman, 1989; Gurman et al., 1984, 1986), using methodology described in detail in previous papers from this laboratory (Blackburn et al., 1991; Sanyal et al., 1993; Strange et al., 1987). The parameters refined in the fit were as follows: E_0, the photoelectron energy threshold; R_i, the distance from Cu to atom i; and $2\sigma^2_i$, the Debye−Waller term for atom i. For the protein fits, the coordination numbers were allowed to vary but were constrained so as to produce Debye−Waller factors within reasonable limits (first shell, $0 < 2\sigma^2 < 0.012$; second shell, $0.005 < 2\sigma^2$). Multiple-scattering contributions from outer-shell (C_2, C_3, N_4, and C_5) atoms of coordinated histidine rings were simulated using well-documented methodology described in previous papers from this laboratory (Blackburn et al., 1991; Sanyal et al., 1993; Strange et al., 1987). The quality of the fits was determined using a least-squares fitting parameter, F, defined as

$$F^2 = (1/N)\sum k^6(\chi_i^{\text{theor}} - \chi_i^{\text{exp}})^2$$

referred to as the fit index.

RESULTS AND DISCUSSION

Copper Stoichiometry. Bifunctional α-AE was found to contain less than 0.2 Cu per mole of enzyme as isolated. This suggests that, like DβM (Blackburn et al., 1988), the copper is rather weakly bound in the active sites of the monooxygenase domain. To reconstitute the enzyme with copper, we adopted a procedure developed for the DβM system which uses phosphate to buffer the added copper at concentrations in the 0.1−1 μM level via the formation of sparingly soluble Cu^{2+}−phosphate complexes. After addition of 2 molar equiv of $^{63}Cu^{2+}$ to the enzyme in 50 mM phosphate buffer, the sample was washed with the phosphate buffer containing a low concentration (5 μM) of $^{63}Cu^{2+}$ which provided sufficient background concentration of free metal ion to prevent equilibrium dissociation of Cu^{2+} from the enzyme but was low enough not to interfere with spectroscopic measurements. Application of this protocol to two independent samples of α-AE gave values of the Cu/protein ratio of 2.2 and 2.4 ± 0.2. These results agree well with those of Miller et al. (1992), in which a functional requirement for 2 coppers per protein was demonstrated.

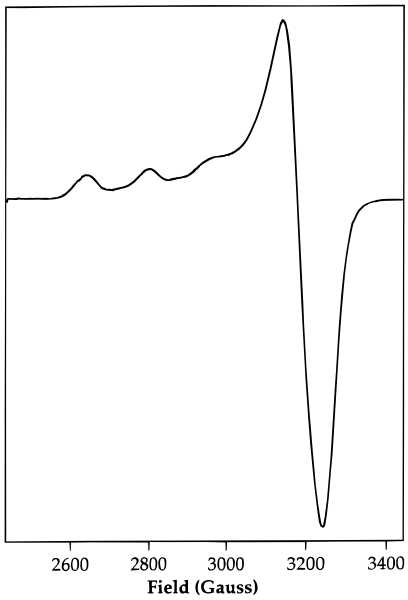

FIGURE 2: EPR spectrum of $^{63}Cu^{2+}$-reconstituted α-AE. Instrumental parameters were as follows: frequency = 9.11 GHz, modulation amplitude = 10 G, gain = 1.25×10^3, and $T = 120$ K.

EPR Spectroscopy. Figure 2 shows the EPR spectrum of the fully reconstituted α-AE. Two independent reconstitution experiments on independent samples gave superimposable spectra. Double integration and comparison to a Cu(II)−EDTA standard indicates that 98 ± 13% of the total copper is EPR detectable. Thus, the spectrum is representative of mononuclear Cu(II) sites with no magnetic coupling or residual Cu(I) component. The g and A values, derived by inspection ($g_{||} = 2.25$, $g_{\perp} = 2.05$, $A_{||} = 162$ G), are typical of tetragonally coordinated Cu(II) sites with O and/or N donor ligands and are close to those recently reported for the copper centers in the isolated monooxygenase domain ΔProPHMs-382 (Eipper et al., 1995). The EPR parameters differ somewhat from those reported by Freeman et al. (1993) ($g_{||} = 2.29$, $A_{||} = 142$ G) for the bifunctional α-AE, but the reasons for this discrepancy are not clear. Visual inspection of the spectrum suggests a single EPR species, but attempts at simulation using a single set of g and A values do not produce an entirely satisfactory fit (data not shown). This may suggest that the spectrum represents the combination of two similar but nonequivalent Cu(II) sites (*vide infra*). Further simulations are in progress to test this hypothesis.

X-ray Absorption Spectroscopy (XAS). EXAFS and absorption edge studies are useful techniques for determining structural information on the local environment of metal ions in proteins. Unlike EPR, both oxidation states of copper are amenable to study by XAS, which provides a powerful method for charting structural changes accompanying the catalytically significant redox cycling events. In this study,

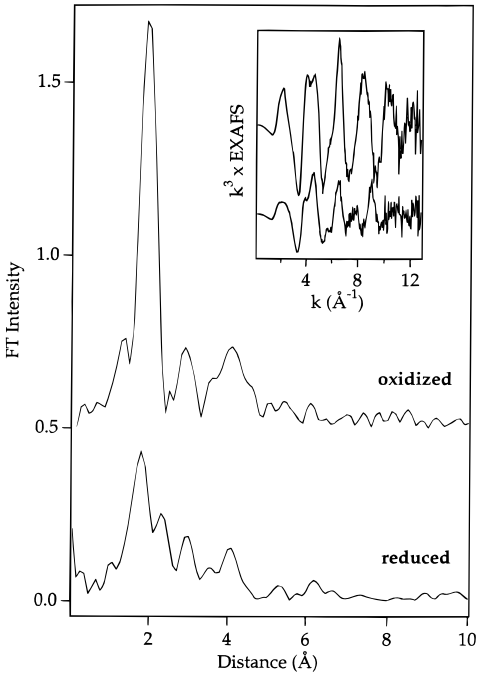

FIGURE 3: Comparison of Cu K-EXAFS and Fourier transforms of oxidized (top) and reduced (bottom) α-AE.

we have investigated the EXAFS and edges of oxidized, reduced, and substrate-bound-reduced forms of α-AE. A comparison of the raw data for oxidized and reduced enzyme forms is given in Figure 3. Inspection of these data, particularly the Fourier transforms, indicates that major structural changes accompany reduction of oxidized enzyme, while binding of substrate to the reduced form produces only minimal structural perturbation. A detailed analysis of the EXAFS data has been carried out using curved-wave, multiple-scattering theory.

EXAFS. The EXAFS data for the oxidized enzyme are typical of Cu(II)−imidazole coordination. The FT shows a major intense peak at $R \sim 2.0$ Å, together with minor peaks at $R \sim 3.0$ and 4.0 Å. This pattern has been well-documented as arising from the Cu−N_α, Cu−C_β, and Cu−C_γ/N_γ atoms of the coordinated imidazole ligand(s), respectively. Since the C−N_α−C_γ/N_γ angle is ∼163°, the near colinearity of the triatom groups leads to significant multiple-scattering (MS) interactions which serve as a fingerprint for imidazole (histidine) coordination. Quantitative analysis of the MS contribution can provide an estimate of the number of histidine ligands coordinated to the Cu(II) centers (Blackburn et al., 1991; Fan et al., 1995; Reedy & Blackburn, 1994; Strange et al., 1987).

Acceptable fits to the unfiltered EXAFS data of α-AE have been obtained for average (per Cu) coordination environments of the form $Cu(His)_x(O/N)_{4-x}$, with x between 2 and 3, as shown in Figure 4. This corresponds to an average 4-coordinate Cu(II) environment with 2−3 histidine ligands per Cu and the remainder non-histidine O or N donor ligands, most probably corresponding to solvent O atoms. Parameter sets corresponding to 2-, 2.5-, and 3-His fits are given in Table 2, together with the corresponding values of the least-squares residual or fit index (FI). The fit index is lowest for the 2-His fit (1.30), with slightly larger values for the 2.5-His (1.39) and 3-His (1.49) fits, respectively. The values of the fit indices are too close to allow meaningful distinction in the goodness of fit, and the fits differ only in the magnitude

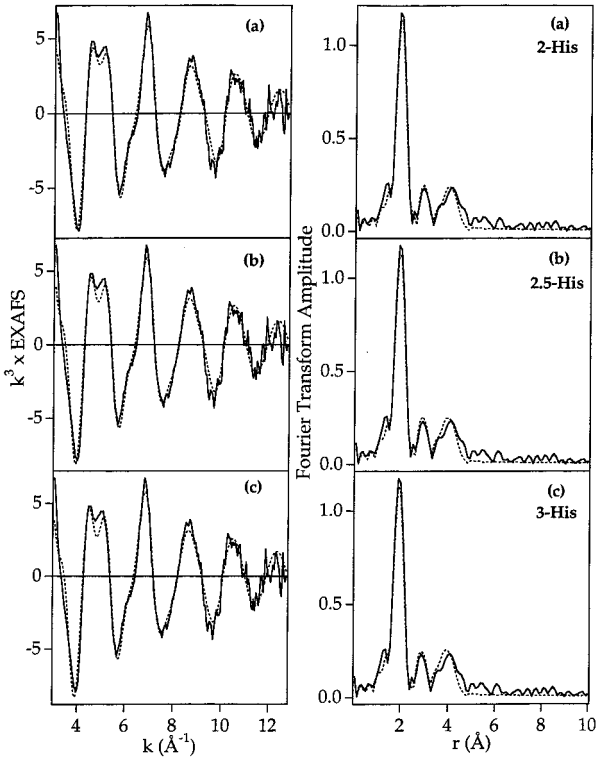

FIGURE 4: Experimental versus simulated Cu K-EXAFS and Fourier transforms of oxidized α-AE: top panel, 2-histidine fit; middle panel, 2.5-histidine fit; and bottom panel, 3-histidine fit. Parameters used to generate the simulations are given in Table 2.

of the Debye−Waller terms for the outer-shell imidazole C and N atoms. In previous studies on Cu(II)−His systems, we have consistently noted that the DW terms for the second-shell Cu−C_β interactions are approximately double those of the first-shell Cu−N_α interactions. This empirical observation would tend to favor the 2.5 His per Cu fit. Another reason for favoring the 2.5-His fit is the fact that there are only 5 conserved His residues between the catalytic cores of DβM and PHM: H^{107}, H^{108}, H^{172}, H^{242}, and H^{244}. If all 5 His residues coordinate, and nonhomologous His coordination is excluded, then the average His coordination per copper must be 2.5. Support for coordination of H^{108} and H^{244} has recently been obtained from site-directed mutagenesis. However, this reasoning will remain speculative until mutagenesis experiments have been carried out on all 5 conserved His residues. In the meantime, the EXAFS analysis provides firm evidence for 4 O/N ligands per Cu at 1.97 ± 0.02 Å, with 2−3 of these ligands being histidines.

The Cu(I) form of α-AE is expected to be the form that binds dioxygen and activates it for hydroxylation of the peptide substrate. Structural characterization of the Cu(I) form is thus pivotal for understanding the monooxygenase mechanism at the molecular level. XAS is unique in its ability to provide structural information on the Cu(I) centers, and comparison with data on the oxidized form gives valuable insights into the catalytic role of the copper centers. As shown in Figure 3 above, ascorbate reduction of α-AE leads to a dramatic change in structure, exemplified by a large (<2-fold) decrease in the amplitude of the first shell in the FT and the appearance of a well-resolved splitting of the first shell into two peaks at $R = 1.90$ and 2.3 Å, respectively. Detailed simulations show that these changes can be interpreted by the loss of the non-imidazole O/N shell, a decrease in the average Cu−imidazole bond length to 1.91

Table 2: Parameters Used To Simulate the EXAFS and Fourier Transforms of Oxidized α-AE[a]

first shell			outer shells			
shell	R (Å)	$2\sigma^2$ (Å^2)	shell	R (Å)	∠Cu−N$_\alpha$−X (deg)	$2\sigma^2$ (Å^2)
			Fit A: 2 Histidines, 2 O/N, FI = 1.30			
2 N$_\alpha$ (imid)	1.97	0.006				
2 O/N	1.97	0.006				
			2 C$_\beta$ (imid)	2.82	−132	0.008
			2 C$_\beta$ (imid)	2.92	122	0.008
			2 C$_\gamma$/N$_\gamma$ (imid)	4.03	158	0.015
			2 C$_\gamma$/N$_\gamma$ (imid)	4.13	−168	0.015
			Fit B: 2.5 Histidines, 1.5 O/N, FI = 1.39			
2.5 N$_\alpha$ (imid)	1.97	0.006				
1.5 O/N	1.97	0.006				
			2.5 C$_\beta$ (imid)	2.82	−132	0.011
			2.5 C$_\beta$ (imid)	2.92	122	0.011
			2.5 C$_\gamma$/N$_\gamma$ (imid)	4.03	158	0.020
			2.5 C$_\gamma$/N$_\gamma$ (imid)	4.13	−168	0.020
			Fit C: 3 Histidines, 1 O/N, FI = 1.49			
3 N$_\alpha$ (imid)	1.97	0.006				
1 O/N	1.97	0.006				
			3 C$_\beta$ (imid)	2.82	−132	0.015
			3 C$_\beta$ (imid)	2.92	122	0.015
			3 C$_\gamma$/N$_\gamma$ (imid)	4.03	158	0.025
			3 C$_\gamma$/N$_\gamma$ (imid)	4.13	−168	0.025

[a] Estimated errors are ±25% for coordination numbers, ±0.02 Å for first-shell distances, and ±0.05 Å for outer-shell distances. Debye−Waller terms ($2\sigma^2$) are highly correlated with coordination numbers, and no independent estimation of their errors is possible.

± 0.02 Å, and the appearance of a new Cu(I)−ligand interaction at 2.27 ± 0.02 Å, best simulated by a second-row scatterer such as S or Cl. Inclusion of a shell of 2 ± 1 C atoms at 3.24 Å, in addition to the outer-shell C atoms from the imidazole rings, lowered the fit index from 0.69 to 0.42. These C atoms could arise from the C$_\beta$ (methylene) and/or C$_\delta$ (methyl) atoms of a methionine ligand (see below). These observations are reminiscent of the change in coordination that accompanies reduction of DβM (Blackburn et al., 1991; Reedy & Blackburn, 1994; Scott et al., 1988), where S coordination has been demonstrated at the Cu$_B$ (dioxygen-binding) site. However, the second-row scatterer component of the amidating enzyme appears more intense and even better resolved than observed in DβM. The best fit to the reduced data is shown in Figure 5a, and the parameter set corresponding to this simulation is given in Table 3. Since it is unlikely that reduction elicits dissociation of coordinated histidine ligands, we have simulated the data with an average of 2.5 His per Cu(I). As expected from the 25% error inherent in the determination of coordination numbers from EXAFS analysis, fits involving 2 His per Cu(I) were equally acceptable. On the other hand, 3-His fits were unable to reproduce the very low amplitude of the first shell unless unreasonably large DW terms were employed, which suggests an upper limit of 2.5 His per copper. In support of this conclusion, the average Cu−His bond length is short (1.91 Å), again suggestive of 3-coordination or lower at each copper. The S/Cl interaction fits well to 0.5 S at 2.27, indicative of Cu−S/Cl coordination at 1 of the 2 Cu(I) centers. Thus, neither Cu can have more than 3 His ligands if the overall average coordination number is ≤3.

The effect of substrate binding to the reduced enzyme is shown in Figure 5b. Structural perturbation is minimal, although small differences are observed in the EXAFS data which can be traced to a decrease in the DW term for the S/Cl shell. The parameters used in the simulation are given in Table 3 and indicate that the major effect is a decrease in the DW for the S shell from 0.009 to 0.004 Å^2. A reasonable

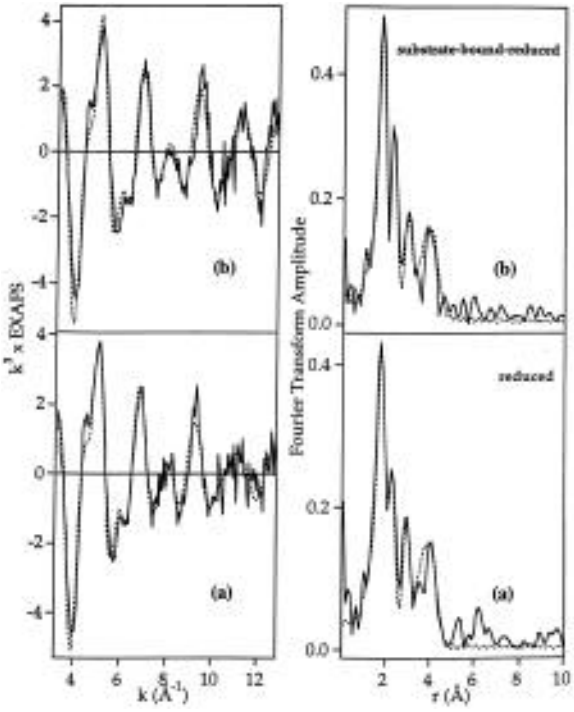

FIGURE 5: Experimental versus simulated Cu K-EXAFS and Fourier transforms of reduced forms of α-AE: bottom panel, reduced enzyme; and top panel, substrate-bound-reduced enzyme. Parameters used to generate the simulations are given in Table 3.

interpretation of this finding is that binding of substrate strengthens the Cu−S/Cl interaction, most likely via locking the active site in a more rigid conformation. On the other hand, no additional scatterers are observed in the EXAFS of the substrate-bound form, implying that peptide binds close to the Cu(I) but does not coordinate.

Absorption Edges. Figure 6 shows the absorption K-edges for oxidized, reduced, and substrate-bound-reduced enzyme. The edge profile of the oxidized enzyme is typical of tetragonally coordinated Cu(II) with a midpoint energy of

Table 3: Parameters Used To Simulate the EXAFS and Fourier Transforms of Reduced and Substrate-Bound-Reduced α-AE, with the Average Histidine Coordination Number Fixed at 2.5 per Copper[a]

first shell			outer shells			
shell	R (Å)	$2\sigma^2$ (Å^2)	shell	R (Å)	∠Cu−N_α−X (deg)	$2\sigma^2$ (Å^2)
			Reduced, FI = 0.426			
2.5 N_α (imid)	1.91	0.016				
0.5 S (met)	2.27	0.009				
			2.5 C_β (imid)	2.85	−122	0.015
			2.5 C_β (imid)	2.95	132	0.015
			2.5 C_γ/N_γ (imid)	4.10	168	0.030
			2.5 C_γ/N_γ (imid)	4.20	−158	0.030
			2 C	3.24		0.022
			Reduced plus Substrate (N-acetyl-Tyr-Val-Gly), F = 0.604			
2.5 N_α (imid)	1.90	0.016				
0.5 S (met)	2.27	0.004				
			2.5 C_β (imid)	2.85	−122	0.015
			2.5 C_β (imid)	2.95	132	0.015
			2.5 C_γ/N_γ (imid)	4.10	168	0.030
			2.5 C_γ/N_γ (imid)	4.20	−158	0.030
			2 C	3.24		0.022

[a] Estimated errors are ±25% for coordination numbers, ±0.02 Å for first-shell distances, and ±0.05 Å for outer-shell distances. Debye−Waller terms ($2\sigma^2$) are highly correlated with coordination numbers, and no independent estimation of their errors is possible.

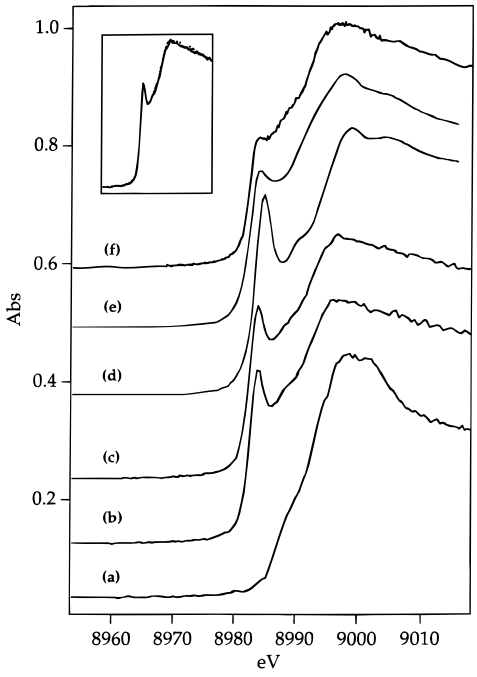

FIGURE 6: Cu K-absorption edges of oxidized and reduced forms of α-AE and related systems: (a) oxidized α-AE, (b) reduced α-AE, (c) substrate-bound-reduced α-AE, (d) 2-coordinate bis(1,2-dimethylimidazole)copper(I), (e) 3-coordinate tris(1,2-dimethylimidazole)copper(I), and (f) reduced DβM. The inset is an overlay of the absorption edges of reduced and substrate-bound-reduced α-AE.

~9000 eV. A weak inflection point is observed on the absorption edge at 8988 eV. Such features are often observed in 5-coordinate Cu(II) systems (Sanyal et al., 1993). On the other hand, no intense feature attributable to 1s → 4p + shakedown (Smith et al., 1985; Strange et al., 1990) characteristic of square planar Cu(II) is observed. Thus a 5-coordinate or distorted 4-coordinate geometry seems likely. Although only four strong scatterers are required to simulate the EXAFS, this does not preclude the presence of a fifth axial ligand. In fact, axial ligation is seldom detected by EXAFS due to the strong Jahn−Teller distortion and associated large increase in the Debye−Waller term for the weak axial ligand.

The absorption edges of the reduced and substrate-bound-reduced enzyme show an intense edge feature (bound-state transition) at 8983.7 eV. This feature is characteristic of Cu(I) in a coordination environment such as 2-coordinate or trigonal planar 3-coordinate (Blackburn et al., 1989; Sanyal et al., 1993). For example, we recently reported edge data on 2- and 3-coordinate 1,2-dimethylimidazole copper(I) complexes which showed well-resolved edge features at 8984.7 and 8984.0 eV, respectively, shown for comparison in parts d and e of Figure 6. The intense 8984.7 eV peak in the 2-coordinate complex is assigned to the 1s → $4p_{x,y}$ (nonbonding) transition of the linear complex. The transition is also present in the edge spectrum of the 3-coordinate imidazole complex, although its intensity is attenuated considerably. This behavior has been noted previously in 3-coordinate Cu(I)N_3 systems, where the 8984 eV transition has also been assigned to a 1s → $4p_x$ transition (x direction normal to the N_3 plane) (Kau et al., 1987). The intensity of the transition is expected to be less than that of the 2-coordinate complex, since the presence of only one nonbonding orbital reduces the probability of the transition. However, the intensity also correlates with the degree of planarity of the 3-coordinate system (Blackburn et al., 1989). Thus, the intensity decreases with the degree of distortion of the complex from planar (trigonal D_{3h} or T-shaped C_{2v}) toward pyramidal (C_{3v}) geometry where the band is generally present only as a shoulder. A simplistic explanation of this effect supposes that distortion from planarity requires increasing amounts of 4s + $4p_z$ mixing in the excited states and, consequently, makes the transition increasingly forbidden.

The intensity of the 8984 eV edge feature in reduced α-AE approaches that found in the 2-coordinate 1,2-dimethylimidazole complex and exceeds the usual intensities found in nonplanar Cu(I)N_3 systems. Given the clear evidence for an average coordination of 2−2.5 His ligands and 0.5 S ligand per copper from the EXAFS analysis, it is likely that at least 1 of the copper centers (Cu_B) is 3-coordinate with the other (Cu_A) either 2- or 3-coordinate. The intensity of the 8983 eV transition also suggests that the coordination of both Cu(I) centers approaches planarity. An analogous

feature is observed in the K-edge of reduced dopamine β-monooxygenase (Figure 6f), but its intensity is less than that found in the bifunctional α-AE. Thus although the ligation of the sites appears very similar in the reduced forms of the two enzymes, the coordination environment of DβM appears more distorted than that of bifunctional α-AE, and it is possible that the amidating enzyme has 1 fewer coordinated histidine (at Cu_A) than dopamine β-monooxygenase.

Figure 6c shows the K-edge of the substrate-bound-reduced form, and the inset to Figure 6 shows the edges of reduced and substrate-bound-reduced enzymes superimposed. The two edges are identical, leading to the conclusion that substrate binding produces no change in the coordination geometry of the Cu(I) centers. This is in good agreement with the result of the EXAFS study, which indicated that the binding of substrate produced no change in coordination but did seem to lock the S-ligated copper center into a more rigid conformation.

CO Binding. Carbon monoxide has been used extensively as a probe of dioxygen binding to Fe(II) and Cu(I) centers in proteins because of the similarity of its electronic structure and mode of binding. Both ligands have empty antibonding orbitals of π symmetry which interact with filled metal d orbitals to generate back-bonding interactions. In the case of CO, the back-bonding leads to a decrease in the IR stretching frequency which is often highly diagnostic of the coordinate structure of the Cu(I) center. Previous studies have shown that CO binds to only one of the Cu(I) centers in DβM. In the fully metalated enzyme, the ratio of CO/Cu and the S donor coordination number were both found to be 0.5, whereas in the Cu_A-depleted form, both the S coordination number and the CO/Cu ratio increased to 1.0 (Blackburn et al., 1990; Reedy & Blackburn, 1994). These data led to the conclusion that CO bound to only 1 of the 2 copper centers (Cu_B) which was also the site of S coordination (Reedy & Blackburn, 1994). The observation of CO inhibition kinetics, which showed competitive behavior with respect to O_2, established the Cu_B center as the site of dioxygen binding (Blackburn et al., 1990).

We have carried out similar studies on the binding of CO to reduced α-AE with the goal of establishing whether similar chemistry pertains to the Cu(I) centers of the amidating enzyme. The stoichiometry of CO binding to reduced α-AE was determined by the method described in Reedy et al. (1994). A value of 0.52 CO per Cu(I) was determined, establishing that, like DβM, the copper centers of the monooxygenase domain of α-AE are inequivalent and only one of them binds CO. The FTIR spectrum of this carbonyl complex is shown in Figure 7. The intraligand stretching frequency of the coordinated CO occurs at 2093 cm^{-1}, close to that determined for DβM (2089 cm^{-1}).

It is useful to compare this value to the CO stretching frequencies of carbonyl complexes of Cu(I) centers in a number of crystallographically characterized proteins and models. Deoxyhemocyanin (deoxyHc), the oxygen-binding protein of molluscs and arthropds, contains a dinuclear Cu(I) center in which each copper is coordinated to 3 His residues (Hazes et al., 1993). The dinuclear unit binds 1 CO per 2 Cus, with ν(CO) values of 2063, 2053, and 2043 cm^{-1} for molluscan, *Limulus*, and arthropodal Hcs, respectively (Fajer & Alben, 1972). CO also binds to the Cu_B center of heme-copper oxidases [ν(CO) = 2062 cm^{-1} (Thomas et al., 1994)],

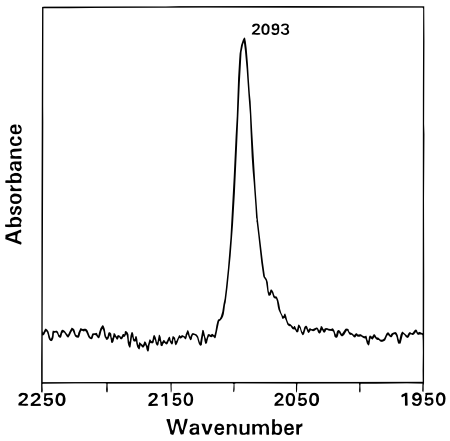

FIGURE 7: FTIR spectrum of the CO complex of ascorbate-reduced α-AE.

the coordination of which is known from biochemical (Hosler et al., 1993), spectroscopic (Fan et al., 1995), and most recently crystallographic (Iwata et al., 1995; Tsukihara et al., 1995) studies to be also comprised of 3 His ligands. While the structure of these protein Cu(I)−carbonyls can only be inferred from the native structures, it is reasonable to propose a 4-coordinate Cu(I)His_3CO structure, especially as CO is known to bind strongly only to 3-coordinate Cu(I) precursor complexes (Pasquali & Floriani, 1984). Thus, in the Cu(I)His_3CO protein systems as well as in a number of Cu(I)N_3CO model complexes [see Table II in Blackburn et al. (1990)], ν(CO) is below 2070 cm^{-1}. As we have argued previously (Blackburn et al., 1990; Pettingill et al., 1991; Reedy & Blackburn, 1994), the ~20 cm^{-1} increase in ν(CO) to the values found in DβM (2089 cm^{-1}) and α-AE (2093 cm^{-1}) is indicative of a decrease in the π-back-bonding interaction from Cu(I) to CO. This would require the Cu(I) center to be less electron-rich than in the Cu(I)N_3 systems described above and suggests either a decrease in Cu(I) coordination number or (more likely) a decrease in the basicity of one or more of the coordinated ligands. Such an effect would be expected to occur if one histidine of a Cu$(His)_3$ site were replaced by the poorer donor methionine. We have recently shown by site-directed mutagenesis (Eipper et al., 1995) that M^{314} is absolutely obligatory to catalytic activity in the ΔPro-PHM382s monooxygenase domain construct. This latter result, the unambiguous evidence from the present work of S coordination, and the high value of ν(CO) argue strongly in favor of M^{314} as the S ligand to Cu(I) in α-AE and other forms of the amidating enzyme.

Structural and Mechanistic Conclusions. The spectroscopic data described in this paper suggest a structural model for the copper centers in bifunctional α-AE very similar to that proposed previously for DβM (Reedy & Blackburn, 1994; Reedy et al., 1995). The important elements of this model are as follows. The enzyme contains 2 coppers per 75 kDa protein molecule, which are located in mononuclear coordination environments. The Cu(II) coordination of the oxidized enzyme is typical of type 2 copper proteins, with 2−3 histidines and 1−2 O/N (probably O from solvent, Asp or Glu) as equatorial ligands. Reduction causes a major structural change. The Cu(I) centers are structurally inequivalent since only one of them binds CO. The non-histidine O/N shell is displaced, and the Cu(I) coordination involves a maximum of 2.5 His ligands together with 0.5 S/Cl ligand per copper. The value of ν(CO) is suggestive

Scheme 1: Structural Model for the Copper Centers in Oxidized, Reduced, and Carbonylated α-AE[a]

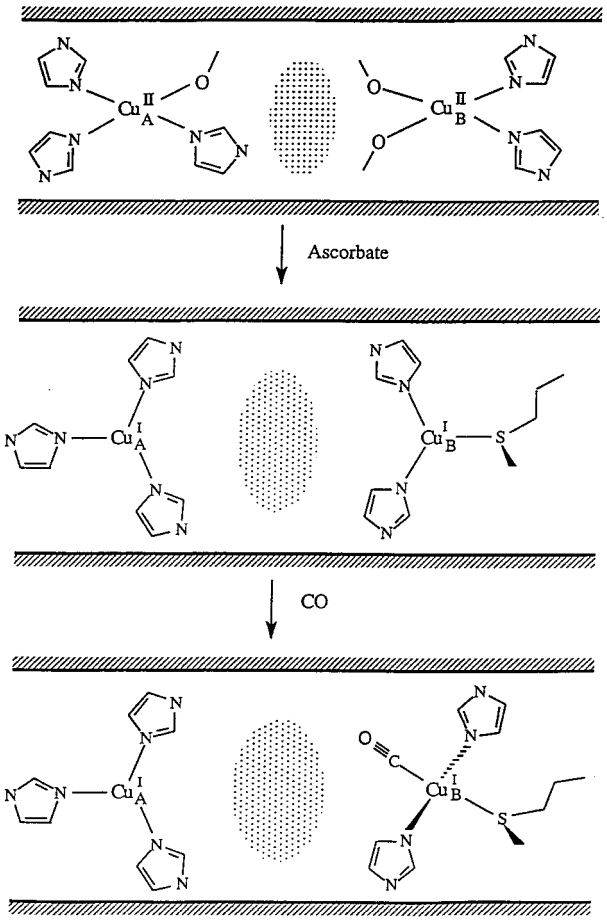

[a] The number of histidines coordinated to Cu_A is shown as 3. However, a model in which Cu_A is coordinated by only 2 histidines is equally consistent with the data.

of coordination of a weak donor such as methionine, which is supported by a previous observation that the ΔPro-PHM382s mutant $M^{314}I$ is totally inactive. Binding of the peptide substrate N-Ac-Tyr-Val-Gly causes minimum structural perturbation at the Cu(I) centers but appears to induce a more rigid conformation in the vicinity of the S-Met ligand. The unusually intense 8983 eV feature in reduced and substrate-bound-reduced enzyme is suggestive of a trigonal planar or digonal coordination environment for Cu(I). The structural model proposed for the copper centers is shown in Scheme 1, which indicates 3 histidines as ligands to Cu^I_A and 2 histidines and 1 methionine as ligands to Cu^I_B. However, in view of the intense 8984 eV edge feature and the lack of CO-binding ability, a 2-coordinate structure for Cu^I_A is also entirely consistent with all the data presented in this paper.

Although we cannot distinguish which Cu(I) center (Cu_A or Cu_B) binds the S-Met ligand, analogy to Dβ M in which S coordination has been shown to occur at the dioxygen/substrate binding site (Blackburn et al., 1990; Reedy & Blackburn, 1994) would suggest a similar conclusion for α-AE and is incorporated into the model shown in Scheme 1. The coordination of a weak donor such as methionine at a Cu(I) dioxygen-binding center is most unusual, since both biomimetic (Karlin & Tyeklar, 1994) and mechanistic (Tian et al., 1994) considerations would favor the presence of stronger donors to help stabilize the formal high-oxidation state which must develop (at least partially) on copper during O−O bond fission. On the other hand, the oxidized (resting) enzyme shows no evidence for methionine coordination (this work) and may indicate that steps in the mechanism that follow formation of the putative Cu(II)−hydroperoxy intermediate may not involve coordinated methionine either. Elucidation of the coordination chemistry of such intermediates is a goal of future studies.

REFERENCES

Bertelsen, A. H., Beaudry, G. A., Galella, E. A., Jones, B. N., Ray, M. L., & Mehta, N. M. (1990) *Arch. Biochem. Biophys. 279*, 87−96.

Binsted, N., Gurman, S. J., & Campbell, J. W. (1988) *EXCURV88 Program*, Daresbury Laboratory, Warrington, U.K.

Blackburn, N. J. (1993) in *Bioinorganic Chemistry of Copper* (Karlin, K. D., & Tyeklar, Z., Eds.) pp 164−183, Chapman & Hall, New York.

Blackburn, N. J., Concannon, M., Khosrow Shahiyan, S., Mabbs, F. E., & Collison, D. (1988) *Biochemistry 27*, 6001−6008.

Blackburn, N. J., Strange, R. W., Reedijk, J., Volbeda, A., Farooq, A., Karlin, K. D., & Zubieta, J. (1989) *Inorg. Chem. 28*, 1349−1357.

Blackburn, N. J., Pettingill, T. M., Seagraves, K. S., & Shigeta, R. T. (1990) *J. Biol. Chem. 265*, 15383−15386.

Blackburn, N. J., Hasnain, S. S., Pettingill, T. M., & Strange, R. W. (1991) *J. Biol. Chem. 266*, 23120−23127.

Davison, A. J., Kettle, A. J., & Fatur, D. J. (1986) *J. Biol. Chem. 261*, 1193−1200.

Eipper, B. A., Mains, R. E., & Glembotski, C. C. (1983) *Proc. Natl. Acad. Sci. U.S.A. 80*, 5144−5148.

Eipper, B. A., Perkins, S. N., Husten, E. J., Johnson, R. C., Keutmann, H. T., & Mains, R. E. (1991) *J. Biol. Chem. 266*, 7827−7833.

Eipper, B. A., Green, C. B. R., Campbell, T. A., Stoffers, D. A., Keutmann, H. T., Mains, R. E., & Ouafik, L. H. (1992) *J. Biol. Chem. 267*, 4008−4015.

Eipper, B. A., Quon, A. S. W., Mains, R. E., Boswell, J. S., & Blackburn, N. J. (1995) *Biochemistry 34*, 2857−2865.

Fajer, L. Y., & Alben, J. O. (1972) *Biochemistry 11*, 4786−4792.

Fan, Y. C., Ahmed, I., Blackburn, N. J., Boswell, J. S., Verkhovskaya, M. L., Hoffman, B. M., & Wikstrom, M. (1995) *Biochemistry 34*, 10245−10255.

Freeman, J. C., Villafranca, J. J., & Merkler, D. J. (1993) *J. Am. Chem. Soc. 115*, 4923−4924.

George, G. N. (1990) *EXAFSPAK Program*, Stanford Synchrotron Radiation Laboratory, Stanford, CA.

Gurman, S. J. (1989) in *Synchrotron Radiation and Biophysics* (Hasnain, S. S., Ed.) pp 9−42, Ellis Horwood Ltd., Chichester, U.K.

Gurman, S. J., Binsted, N., & Ross, I. (1984) *J. Phys. C: Solid State Phys. 17*, 143−151.

Gurman, S. J., Binsted, N., & Ross, I. (1986) *J. Phys. C: Solid State Phys. 19*, 1845−1861.

Hazes, B., Magnus, K. A., Bonaventura, C., Bonaventura, J., Dauter, Z., Kalk, K. H., & Hol, W. G. (1993) *Protein Sci. 2*, 597−619.

Hosler, J. P., Ferguson-Miller, S., Calhoun, M. W., Thomas, J. W., Hill, J., Lemieux, L., Ma, J., Georgiou, C., Fetter, J., Shapleigh, J., Tecklenburg, M. M. J., Babcock, G. T., & Gennis, R. B. (1993) *J. Bioenerg. Biomembr. 25*, 121−136.

Husten, E. J., & Eipper, B. A. (1991) *J. Biol. Chem. 266*, 17004−17010.

Husten, E. J., Tausk, F. A., Keutmann, H. T., & Eipper, B. A. (1993) *J. Biol. Chem. 268*, 9709−9717.

Iwasaki, Y., Kawahara, T., Shimoi, H., Suzuki, K., Ghisalba, O., Kangawa, K., Matsuo, H., & Nishikawa, Y. (1991) *Eur. J. Biochem. 201*, 551−559.

Iwasaki, Y., Shimoi, H., Saiki, H., & Nishikawa, Y. (1993) *Eur. J. Biochem. 214*, 811−818.

Iwata, S., Ostermeier, C., Ludwig, B., & Michel, H. (1995) *Nature 376*, 660−669.

Jones, B. N., Tamburini, P. P., Consalvo, A. P., Young, S. D., Lovato, S. J., Gilligan, J. P., Jeng, A. Y., & Wennogle, L. P. (1988) *Anal. Biochem. 168*, 272−279.
Karlin, K. D., & Tyeklar, Z. (1994) *Adv. Inorg. Chem. 9*, 123−172.
Kau, L. S., Spira-Solomon, D., Penner-Hahn, J. E., Hodgson, K. O., & Solomon, E. I. (1987) *J. Am. Chem. Soc. 109*, 6433−6422.
Kulathila, R., Consalvo, A. P., Fitzpatrick, P. F., Freeman, J. C., Snyder, L. M., Villafranca, J. J., & Merkler, D. J. (1994) *Arch. Biochem. Biophys. 311*, 191−195.
Matthews, D. E., Piparo, K. E., Burkett, V. H., & Pray, C. C. (1994) in *Animal Cell Technology: Products of Today, Prospects for Tomorrow* (Spier, R. E., Griffiths, J. B., & Berthold, W., Eds.) pp 315−319, Butterworth-Heinemann Ltd., Oxford, U.K.
Merkler, D. J., & Young, S. D. (1991) *Arch. Biochem. Biophys. 289*, 192−196.
Merkler, D. J., Kulathila, R., Consalvo, A. P., Young, S. D., & Ash, D. E. (1992a) *Biochemistry 31*, 7282−7288.
Merkler, D. J., Kulathila, R., Tamburini, P. P., & Young, S. D. (1992b) *Arch. Biochem. Biophys. 294*, 594−602.
Milgram, S. L., Johnson, R. C., & Mains, R. E. (1992) *J. Cell Biol. 117*, 717−728.
Miller, D. A., Sayad, K. U., Kulathila, R., Beaudry, G. A., Merkler, D. J., & Bertelsen, A. H. (1992) *Arch. Biochem. Biophys. 298*, 380−388.
Noguchi, M., Seino, H., Kochi, H., Okamoto, H., Tanaka, T., & Hirama, M. (1992) *Biochem. J. 283*, 883−888.
Pasquali, M., & Floriani, C. (1984) in *Copper Coordination Chemistry, Biochemical and Inorganic Perspectives* (Karlin, K. D., & Zubieta, J., Eds.) pp 311−330, Adenine Press, New York.
Pettingill, T. M., Strange, R. W., & Blackburn, N. J. (1991) *J. Biol. Chem. 266*, 16996−17003.
Reedy, B. J., & Blackburn, N. J. (1994) *J. Am. Chem. Soc. 116*, 1924−1931.
Reedy, B. J., Murthy, N., Karlin, K. D., & Blackburn, N. J. (1995) *J. Am. Chem. Soc. 117*, 9826−9831.
Robertson, J. G., Adams, G. W., Medzihradsky, K. F., Burlingame, A. L., & Villafranca, J. J. (1994) *Biochemistry 33*, 11563−11575.
Sanyal, I., Karlin, K. D., Strange, R. W., & Blackburn, N. J. (1993) *J. Am. Chem. Soc. 115*, 11259−11270.
Scott, R. A., Sullivan, R. J., DeWolf, W. E., Jr., Dolle, R. E., & Kruse, L. I. (1988) *Biochemistry 27*, 5411−5417.
Shimoi, H., Kawahara, T., Suzuki, K., Iwasaki, Y., Jeng, A. Y., & Nishikawa, Y. (1992) *Eur. J. Biochem. 209*, 189−194.
Smith, T. A., Penner-Hahn, J. E., Berding, M. A., Doniach, S., & Hodgson, K. O. (1985) *J. Am. Chem. Soc. 107*, 5945−5955.
Southan, C., & Kruse, L. I. (1989) *FEBS Lett. 255*, 116−120.
Stewart, L. C., & Klinman, J. P. (1988) *Annu. Rev. Biochem. 57*, 551−592.
Stoffers, D. A., Barthel-Rosa Green, C., & Eipper, B. A. (1989) *Proc. Natl. Acad. Sci. U.S.A. 86*, 735−739.
Stoffers, D. A., Ouafik, L. H., & Eipper, B. A. (1991) *J. Biol. Chem. 266*, 1701−1707.
Strange, R. W., Blackburn, N. J., Knowles, P. F., & Hasnain, S. S. (1987) *J. Am. Chem. Soc. 109*, 7157−7162.
Strange, R. W., Alagna, L., Durham, P., & Hasnain, S. S. (1990) *J. Am. Chem. Soc. 112*, 4265−4268.
Suzuki, K., Ohta, M., Okamoto, M., & Nishikawa, Y. (1993) *Eur. J. Biochem. 213*, 93−98.
Thomas, J. W., Calhoun, M. W., Lemieux, L. J., Puustinen, A., Wikstrom, M., Alben, J. O., & Gennis, R. B. (1994) *Biochemistry 33*, 13013−13021.
Tian, G., Berry, J. A., & Klinman, J. P. (1994) *Biochemistry 33*, 226−234.
Tsukihara, T., Aoyama, H., Yamashita, E., Tomizaki, T., Yamaguchi, H., Shinzawa-Itoh, K., Nakashima, R., Yaono, R., & Yoshikawa, S. (1995) *Science 269*, 1069−1074.
Zabriskie, T. M., Cheng, H., & Vederas, J. C. (1991) *J. Chem. Soc., Chem. Commun.*, 571−572.

BI960742Y